



## Hyper Swollen Perfluorinated Smectic Liquid Crystal by Perfluorinated Oils

Journal:	<i>RSC Advances</i>
Manuscript ID:	RA-ART-10-2014-012938.R1
Article Type:	Paper
Date Submitted by the Author:	19-Nov-2014
Complete List of Authors:	Murase, Masatsugu; Kyoto University, Department of Physics Takanishi, Yoichi; Kyoto University, Department of Physics Nishiyama, Isa; Dainippon Ink and Chemicals Incorporated, Information Materials Development Centre Yoshizawa, Atsushi; Hirosaki University, Department of Frontier Materials Chemistry Yamamoto, Jun; Kyoto University, Department of Physics

## Hyper Swollen Perfluorinated Smectic Liquid Crystal by Perfluorinated Oils

Masatsugu MURASE<sup>1</sup>, Yoichi TAKANISHI<sup>1</sup>, Isa NISHIYAMA<sup>2</sup>, Atsushi YOSHIZAWA<sup>3</sup> and Jun YAMAMOTO<sup>1</sup>

<sup>1</sup> Department of Physics, Kyoto University, Kitashirakawaoiwake-cho, Sakyo-ku, Kyoto, 606-8502, Japan

<sup>2</sup> DIC Corp. Komuro, Ina-machi, Kitaadachi-gun, Saitama 362-8577, Japan

<sup>3</sup> Department of Frontier Materials Chemistry, Graduate School of Science and Technology, Hirosaki University, 3 Bunkyo-cho, Hirosaki, Aomori 036-8561

Abstract:

We studied the hyper-swollen behavior of a perfluorinated smectic liquid crystal, 11-(4'-cyanobiphenyl-4-yloxy)undecyl pentadecafluorooctanoate (BI), through addition of perfluorinated oils. The studied compound, BI, has a bilayer SmA–SmC phase sequence due to microphase separation of hydrocarbon chains and perfluorinated chains. We found that BI can be diluted with straight-chain, soft perfluorinated oils and that the repeat distance of the smectic layer can be greatly swollen to about three times thicker than that of pure BI. However, there was no clear physical mechanism for the long-range interlayer repulsive forces, such as the electrostatic force, observed in the lyotropic system. Furthermore, we found that interlayer tilting can be propagated along the smectic layers in the SmC phase even in the hyper-swollen state, despite insertion of thick liquid layers of perfluorinated oil between the smectic layers of BI. The orientation of the intercalated perfluorinated oils was also discussed based on the conoscope observation.

## Introduction

Liquid crystals (LCs) are frequently categorized by whether the phase transition from isotropic liquid to crystal phases is temperature dependent (thermotropic LCs) or controlled by a solvent (lyotropic LCs). Thermotropic LCs are mainly stabilized by the change in entropy associated with the excluded volume, while lyotropic LCs exhibit a high degree of microscopic segregation called microphase separation. Amphiphilic molecules are easily arranged into lyotropic LC phases through mixing with a solvent such as water. Because they have both hydrophilic and hydrophobic groups, amphiphilic molecules can be stably and microscopically separated with solvents.

In conventional lyotropic lamellar phases, such as multi-layered lipid membranes, Van der Waals attraction and hydration repulsion forces are balanced when the thickness of the intercalated fluid layer is nearly the same as that of the membrane, so that the swelling limit is close to the volume fraction of the solvent ( $\phi$ ) of  $\sim 0.5$ . An additional long-range repulsive force is required to greatly expand the interlayer spacing, such as the electrostatic force [1] or Helfrich fluctuation force [2].

In thermotropic LC systems, swelling behavior associated with solvents have recently been investigated [3–6]. Most of these solvents were n-alkanes with a maximum swelling rate

of 1.5. To study the lyotropic-like microseparation effect of solvents on thermotropic LC phase behavior, a perfluorinated moiety was introduced into the conventional LC molecule, cyanobiphenyl. Thus, a perfluorinated thermotropic LC, 11-(4'-cyanobiphenyl-4-yloxy)undecyl pentadecafluorooctanoate (BI), was synthesized [7]. This compound has both perfluorinated and hydrocarbon chains (Fig. 1). Because there is limited solubility between the perfluorinated and hydrocarbon chains, the BI molecule is considered an amphiphilic molecule. BI is expected to have both thermotropic and lyotropic properties and to exhibit novel functions and/or structures through competition or frustration between these properties.

In this study, we mixed perfluorinated oils with BI and investigated swelling behavior as in a lyotropic system using X-ray diffraction and conoscope measurements. We also evaluated interlayer correlation of the tilt direction in the SmC phase, because in the hyper-swollen state, a large amount of *isotropic* perfluorinated oil is present between the thermotropic *anisotropic* smectic mesogens.

## Experimental

The chemical structure and phase sequence of BI is shown in Fig. 1. It has a hydrocarbon

chain near the core and a perfluorinated chain at the peripheral end. For the mixing study, three perfluorinated oils were used. Two (Fo\_a and Fo\_b) were straight chain-like, while the other (Fo\_c) had a less anisotropic ring-shaped structure (Figs. 1(b)–(d)). Because the perfluorinated oils readily evaporated, most of the measurements for the mixtures were carefully operated in the heating process. We observed that BI and Fo\_a(b,c) were more miscible with each other in SmA than in the isotropic state. Thus, the heating process was suitable to avoid macroscopic phase separation. The mixture could not be maintained for a long time at high temperatures due to evaporation of the oils and macroscopic phase separation. To ensure that evaporation of oils or macroscopic phase separation did not occur, the phase transition temperature was consistently checked and confirmed as stable during each measurement.

Optical microscope observation was performed using a polarized microscope (BX51; Olympus) equipped with a charge-coupled device (CCD) camera (U-CMAD3; Olympus) and DVD recorder (RDZ-D87; Sony). The temperature of the sample was controlled using an LK-600PH (Linkam Scientific Instruments). We prepared the samples by sandwiching the mixtures between a slide glass and cover glass without surface treatment. X-ray diffraction (XRD) patterns of the samples were obtained using a real-time X-ray diffractometer (D8

Discover; Bruker AXS GmbH) and a small-angle X-ray system (MicroMax-007HF; Rigaku) equipped with a hot stage and a temperature controller [8,9]. Samples were sandwiched between convex lenses or inserted into closed glass capillaries to prevent evaporation of the fluorinated oils and placed in a hand-made temperature-stabilized holder ( $\pm 0.1$  °C). During the X-ray measurement, the texture of the samples was observed using a hand-made microscope and the phase transition was confirmed visually.

In the XRD using D8 Discover, the tube voltage and current of the X-ray generators were 45 kV and 20 mA, respectively, and a parallel Cu K $\alpha$  X-ray beam generated by a cross-coupled Göbel mirror was used to irradiate the sample. The diffraction pattern was obtained using a two-dimensional position-sensitive proportional counter (PSPC) detector (Hi-Star; Bruker AXS GmbH) at a camera distance of 300 mm for a counting time of 60–300 s. In the small-angle X-ray system (MicroMax–007HF), the tube voltage and current of the X-ray generators were 40 kV and 20 mA, respectively, and the Cu K $\alpha$  X-ray beam was generated by a confocal mirror. The diffraction pattern was obtained using a cooled CCD camera (C9299-01; Hamamatsu Photonics KK) with an image intensifier (Hamamatsu Photonics KK) at a camera distance of  $\sim 750$  mm for a counting time of 60 s–10 min.

Conoscope observation was performed using a He-Ne laser with a wavelength of 632.8

nm expanded to a diameter of  $\sim 10$  mm with a beam expander, focused on the middle of a 250- $\mu\text{m}$ -thick homeotropic cell using an objective lens with an extra-long working distance and large numerical aperture (0.45). The 250- $\mu\text{m}$ -thick homeotropic cell was placed in a hand-made oven controlled by a temperature controller (E5AK; Omron) and the oven was placed between the crossed polarizers. The conoscope images were projected onto a screen  $\sim 100$  mm from the homeotropic cell and recorded using a video camera. The optical birefringence was determined from the periodicity of the isochromatic circles in the conoscope images based on ref.[10].

## Results and Discussion

Figure 2 shows photographs of pure BI and a mixture with 66.6 wt% Fo<sub>a</sub> at various temperatures under the crossed-Nicols polarizing microscope. Despite the lack of surface treatment on the glass substrate, good homeotropic alignment was spontaneously obtained. For pure BI, a uniform dark texture, due to the optically uniaxial property of homeotropic alignment, was observed below the phase transition temperature to the isotropic liquid (Fig. 2(a)). Because the planar alignment in another cell showed focal conic texture in which the extinction direction under the crossed polarizers was parallel to the layer normal (inset of Fig.



2(a)), this phase was assigned as the SmA phase. On further cooling, a schlieren texture with four brushes appeared below the SmA phase, indicating optical birefringence, characteristic of the SmC phase (Fig. 2(b)). Thus, we confirmed the phase sequence of Iso-SmA-SmC.

For the BI-Fo<sub>a</sub> mixture, the schlieren texture with four brushes was observed in the lower-temperature region (Fig. 2(c)) as in the pure compound (Fig. 2(b)). On heating to 58 °C, the texture changed to dark with small focal conics, indicating SmA (Fig. 2(d)). At 73 °C, an isotropic liquid phase appeared as dark droplets. On further heating, the isotropic phase of Fo<sub>a</sub> coexisted with the SmA phase of the BI-Fo<sub>a</sub> mixture to 100 °C. Above 100 °C, BI and Fo<sub>a</sub> were again quite miscible, resulting in a homogeneous isotropic phase. The phase transition temperature between SmA and SmC of the BI-Fo<sub>a</sub> mixture differed from that of BI alone, in which no textural change indicating phase separation was observed. In addition, the phase transition temperature was consistent during the heating and cooling processes. These results indicate that BI and Fo<sub>a</sub> were completely miscible in the LC phases during our experiment.

A similar texture was observed for the BI-Fo<sub>b</sub> mixture. In [5], the phase transition temperature between Cryst and SmE (together with IL) was reported to differ between the cooling and heating processes, attributed to phase separation. In our study, however, the

transition temperature between the SmA and SmC phases during the cooling process was confirmed to be the same as that during the heating process. After heating to SmA, we rapidly reduced the temperature so that there was little evaporation of the fluorinated oils. Hence, the reported concern regarding phase separation is not applicable to our study. On the other hand, in the BI-Fo\_c mixture, we did not observe clear coexistence of the Iso and SmA phases at the Iso-SmA phase transition, although the phase sequence of the BI-Fo\_c mixture was the same as that of the other two mixtures.

Figure 3 shows the binary phase diagrams for the three mixtures, determined by texture observations during the heating process. The phase behavior of the BI-Fo\_a and BI-Fo\_b mixtures was nearly the same. When the oil concentration was increased, the phase transition temperature between the isotropic phase and the two-phase region in which the isotropic and SmA phases coexisted slightly increased. On the other hand, all of the phase transition temperatures (Iso-SmA, SmA-SmC, and SmC-Cryst) decreased with increasing Fo\_c concentration and the two-phase region in which the isotropic and the SmA phases coexisted was minimal until the Fo\_c content increased to 66.6 wt%. This difference was likely related to differences in solubility between BI and the various oils and/or the microscopic molecular packing state in the mixtures due to the molecular shape (supported by the X-ray results

discussed below).

Figure 4 shows the temperature dependence of the layer thickness of the three mixtures as determined by small-angle XRD. In pure BI, the layer thickness of SmA was about 50 Å, slightly increasing with decreasing temperature. Because the molecular length for all trans conformations was estimated to be 27 Å, the molecules in the smectic phase formed a slightly interdigitated bilayer structure. The layer thickness in SmA of the BI-Fo\_a(b,c) mixtures also increased with decreasing temperature, but at a higher rate than that of pure BI. The smectic layer of all of the mixtures shrank at the SmA-SmC transition due to molecular tilt [11], except for the mixtures containing more than 50 wt% Fo\_c. The temperature dependence of the layer thickness of SmA in the mixtures with high wt% Fo\_a(b) had two regions. At lower temperatures, the change in the layer thickness with temperature was nearly the same among all of the mixtures. At higher temperatures, the layer thickness at a constant temperature was independent of the mixing ratio (Figs. 4(a) and (b)). The boundary between the two regions corresponded to the temperature at which macroscopic phase separation of the isotropic and SmA phases occurs. Hence, the broken lines in Figs. 4(a) and (b) indicate the swelling limit of the layer with the straight-chain-like perfluorinated oils. In the BI-Fo\_c mixtures, swelling was substantially lower than in the other mixtures (Fig. 4(c)).

The most intriguing observation was the absolute layer thickness as a function of the mixing ratio. The smectic layer thickness monotonically increased with increasing oil concentration and unexpectedly swelled up to three times that of pure BI in the mixtures containing 66.6–69.7 wt% Fo\_a(b). The swelling behavior itself was previously observed in SmC\* and SmCA\* phases in a mixture of 4-(2-methylalkanoyl)phenyl 4'-alkyloxybiphenyl-4-carboxylate (MAP) [12] and n-alkane [6], but in the present system, the swelling ratio was unusually large.

This novel swelling behavior was dependent on the concentration of perfluorinated oil in the lower-temperature region to the left of the swelling limit (Fig. 4, broken line). Thus, we evaluated the differences in the swollen states between the three mixtures. Figure 5 shows the dependence of the layer thickness  $d$  on the volume fraction at various temperatures. These calculations were based on [3] with modification, although the calculations for three-dimensional swelling differ somewhat.  $\Phi_{BI}$  is the volume fraction of BI, defined as follows:

$$\frac{1}{\Phi_{BI}} = \frac{V_{BI} + V_{Fo\_a(b,c)}}{V_{BI}} = 1 + \frac{\rho_{BI}}{\rho_{Fo\_a(b,c)}} \frac{w_{Fo\_a(b,c)}}{w_{BI}} \quad (1)$$

where  $V_{BI}$  and  $V_{Fo\_a(b,c)}$  are the volumes of BI and Fo\_a(b,c), respectively;  $\rho_{BI}$  and  $\rho_{Fo\_a(b,c)}$  are the densities of BI and Fo\_a(b,c), respectively, where  $\rho_{Fo\_a}$ ,  $\rho_{Fo\_b}$ , and  $\rho_{Fo\_c}$  are 1.765, 1.723,

and  $1.941 \text{ g/cm}^3$ , respectively [13–15]; and  $w_{BI}$  and  $w_{Fo\_a(b,c)}$  are the masses of BI and  $Fo\_a(b,c)$ , respectively.

When the fluorinated oils have completely reached their swelling limits in BI one- and three-dimensionally, the swelling ratios can be written as follows:

$$\frac{d}{d_{BI}} = \frac{V_{BI} + V_{Fo\_a(b,c)}}{V_{BI}} = \frac{1}{\Phi_{BI}} \quad (\text{one-dimensional}) \quad (2)$$

$$\frac{d}{d_{BI}} = \left( \frac{V_{BI} + V_{Fo\_a(b,c)}}{V_{BI}} \right)^{1/3} = \left( \frac{1}{\Phi_{BI}} \right)^{1/3} \quad (\text{three-dimensional}) \quad (3)$$

The value of  $\rho_{BI}$  is unknown; however, the maximum swelling ratio of the layer thickness should ideally correspond to Eq. (2). Making this assumption,  $\rho_{BI}$  is estimated to be  $1.55 \text{ g/cm}^3$ . This value appears reasonable, because it is greater than the density of cyanobiphenyl liquid crystals ( $0.98\text{--}1.04 \text{ g/cm}^3$  [16]) and lower than that of n-perfluoroheptane ( $1.745 \text{ g/cm}^3$  [17]). The calculated curves for Eqs. (2) and (3) for  $\rho_{BI} = 1.55 \text{ g/cm}^3$  are shown as **line I** and **curve II**, respectively, in Fig. 5. The obtained data for the BI– $Fo\_b$  mixtures correspond well to **line I**. On the other hand, the data for the BI– $Fo\_c$  mixtures are a better fit to **curve II**. If the oils were isotropically dispersed (three-dimensionally), the data should be similar to **curve II**. Hence, we conclude that the  $Fo\_c$  oil was nearly three-dimensionally mixed within the BI– $Fo\_c$  mixtures.

However, some data points in the higher-temperature region deviated from the dilution

law and were independent of  $\Phi_{\text{Fo}_a(b)}$ , indicated by open symbols. This is because two phases (Iso and SmA) coexisted near the I–SmA transition temperature for the multi-component systems (Fig. 4, broken lines). Furthermore, the BI–Fo<sub>a</sub> mixtures, with longer perfluoro chains, appear to be a better fit to **line I**. Based on these results, we conclude that the straight-chain-like perfluorinated oils tend to swell the smectic layer system one-dimensionally and that these oils are mainly localized between the smectic layers composed of BI molecules (Fig. 5(d)).

As noted above, we found that the smectic layer can be swollen to a maximum of three times the thickness of pure BI in both the SmA and SmC phases, based on the XRD results. In the SmA phase, the molecules are not tilted with respect to the smectic layer plane and the molecular orientation in each layer is uniquely determined. Therefore, we cannot confirm interlayer correlation of the molecular orientation in SmA.

In the SmC phase, interlayer tilting correlation can normally be confirmed by optical birefringence of homeotropic alignment. However, the obtained hyper-swollen SmC state was unanticipated. The SmC phase must have interlayer azimuthal tilting correlation even in such a swollen system, but considering that the perfluorinated oils between the BI layers have isotropic order, it would be difficult to propagate the interlayer tilting correlation as is

normally observed. One possibility simultaneously satisfying interlayer molecular tilting correlation and the existence of an interlayer medium with isotropic order is a de Vries-type smectic phase [18]. However, schlieren texture with optical birefringence and layer shrinkage was observed even in SmC with 66.6 wt% Fo\_a (Fig. 2(d)). Hence, a de Vries-type smectic phase is unlikely, because it should be optically uniaxial in visible light. Another possibility is induced anisotropy in the straight-chain-like perfluorinated oils due to intercalated interactions with the terminal perfluorinated groups of the BI molecules, as predicted for the hyper-swollen SmC\* phase diluted by n-alkane [5].

To confirm whether the perfluorinated oils were oriented, we evaluated the optical anisotropy of the mixtures using a conoscope. Figures 6(a) and (b) show typical conoscope images of the SmA phase (80 °C) of pure BI and the 33.3 wt% Fo\_b mixture, respectively. Unfortunately, good conoscope images could not be obtained of the SmC phase, because many brushes and inversion walls could not be erased. There were fewer isochromatic circles due to the interference fringe in the mixture compared to pure BI, indicating that optical anisotropy was decreased by adding the perfluorinated oil. Figure 7(a) shows the optical birefringence,  $\Delta n$ , as a function of temperature calculated from the conoscope images.  $\Delta n$  of the BI-Fo\_b mixture was nearly independent of temperature and its value was about 70% of

that of pure BI (Fig. 7(b)). Assuming that the thickness of the Fo\_b region was  $\sim 20$  Å (Fig. 5(b)), the ratio of  $\Delta n$  would be about 0.7–0.75 if the Fo\_b region had isotropic order, and  $>0.75$  if the Fo\_b region had anisotropic order, as a first approximation. Because the experimental values in Fig. 7(b) are  $<0.75$ , we conclude that the perfluorinated oil had isotropic order, as expected.

In a lyotropic system, a tilted lamellar phase with optical biaxiality was reported when the solvent concentration was low (0.2–0.36) [19], but the mechanism of the long-range correlation of the tilt direction of the lipid molecules through the intercalated water layers was unclear. Ultimately, we are uncertain how the interlayer tilting correlation was propagated in such a hyper-swollen smectic phase. The remaining possibility is that some of the BI molecules penetrated into the interlayer perfluorinated oil regions and the tilting correlation may have been propagated through interactions between the penetrating BI molecules. Further research will be required to investigate this mechanism thoroughly.

In conclusion, we characterized a perfluorinated smectic liquid crystal (BI) possessing both hydrocarbon and perfluorinated chains, which are incompatible. We investigated the effects of mixing perfluorinated oils into this compound and found that straight-chain-like perfluorinated oils at a concentration of up to three times that of BI can be mixed with BI,



with the smectic layer swelling by up to three times. Moreover, we found that the interlayer tilting correlation is propagated in the SmC phase even in such a hyper-swollen system. Considering that the orientation of the perfluorinated oils was isotropic based on conoscope images, we may have observed a new type of interaction propagating tilting correlation in this hyper-swollen system.

#### Acknowledgments

This work was supported by a Grant-in-Aid for Scientific Research on the Priority Area “Creation of Non-equilibrium Soft Matter Physics” Scientific Research (B), the JSPS Core-to-Core Program “International Research Network for Non-equilibrium Dynamics of Soft Matter,” and the Global COE Program “The Next Generation of Physics, Spun from Universality and Emergence” from the Ministry of Education, Culture, Sports, Science, and Technology (MEXT) of Japan. We are also thankful to Mr. Naoyuki Kamo for assisting us with measurements of the physical properties of the BI-Fo<sub>c</sub> mixture.

## References

- [1] K. Naitoh, Y. Ishii and K. Tsujii, *J. Phys. Chem.*, **95**, 7915 (1991).
- [2] R. Strey, R. Schomäcker, D. Roux, F. Nallet and U. Olsson, *J. Chem. Soc. Faraday Trans.*, **86**, 2253 (1990).
- [3] T. P. Rieker, *Liq. Cryst.*, **19**, 497 (1995).
- [4] Y. Yamaoka, Y. Taniguchi, S. Yasuzuka, Y. Yamamura and K. Saito, *J. Chem. Phys.*, **135**, 044705 (2011).
- [5] T. Miyazawa, Y. Yamamura, M. Hishida, S. Nagatomo, M. Massalska-Arodz and K. Saito, *J. Phys. Chem. B*, **117**, 8293 (2013).
- [6] J. Yamamoto, I. Nishiyama and H. Yokoyama, in preparation.
- [7] JP 2009-21706, I. Nishiyama, H. Ishizuka and A. Yoshizawa
- [8] A. Yoshizawa, A. Nishizawa, K. Takeuchi, Y. Takanishi and J. Yamamoto, *J. Phys. Chem. B*, **114**, 13304 (2010).
- [9] D. Tsuji, Y. Takanishi, J. Yamamoto and A. Yoshizawa, *J. Phys. Chem. C*, **116**, 8678 (2012).
- [10] E. Gorecka, A. D. L. Chandani, Y. Ouchi, H. Takezoe and A. Fukuda, *Jpn. J. Appl. Phys.*, **29**, 131 (1990).
- [11] C. R. Safinya, M. Kaplan, J. Als-Nielsen, R. J. Birgeneau, D. Davidov, J. D. Litster D. L. Johnson and M. E. Neubert, *Phys. Rev. B*, **21**, 4149 (1980)
- [12] A. Yoshizawa, I. Nishiyama, M. Fukumasa, T. Hirai and M. Yamane, *Jpn. J. Appl. Phys.*, **28**, L1269 (1989).
- [13] CAS No. **37486-69-4**
- [14] CAS No. **26738-51-2**
- [15] CAS No. **306-94-5**
- [16] P. E. Cladis, D. Guillon, F. R. Bouchet, and P. L. Finn, *Phys. Rev. A* **23**, 2594 (1981).
- [17] CAS No. **335-57-9**
- [18] J. P. F. Lagerwall and F. Giesselmann, *Chem. Phys. Chem.* **7**, 20 (2006).
- [19] D. C. Wack and W. W. Webb, *Phys. Rev. A* **40**, 2712 (1989).

## Figure Caption

Figure 1 Chemical structures of (a) 11-(4'-cyanobiphenyl-4-yloxy)undecyl pentadecafluorooctanoate (BI), (b) 2H-perfluoro-5,8,11,14-tetramethyl-3,6,9,12,15-pentaoxaoctadecane (Fo\_a), (c) 2H-perfluoro-5,8,11-tetramethyl-3,6,9,12-tetraoxapentadecane (Fo\_b), and (d) perfluorodecalin (Fo\_c).

Figure 2 Microphotographs of (a) SmA and (b) SmC for pure BI, and (c) SmC and (d) SmA for a mixture of BI with 66.6 wt% Fo\_a.

Figure 3 Binary phase diagrams of three mixtures, (a)BI-Fo\_a, (b)BI-Fo\_b, and (c)BI-Fo\_c. The temperatures corresponding to the SmA-SmC phase transition were measured in the cooling process indicated by solid line with closed square symbols, whereas the other temperatures were determined in the heating process. Thus temperatures corresponding to the Cryst.-SmC (or SmA) phase transition measured in the heating process, i.e. the melting points, are indicated by dotted line with open diamond symbols. The liquid crystal phase regions appeared below the melting points indicate the appearance of the monotropic liquid crystal phase.

Figure 4 Temperature dependence of the layer thickness of mixtures with various mixing ratios: (a) BI-Fo\_a (closed triangle, BI:Fo\_a = 1:2; open triangle, BI:Fo\_a = 1:1.5; closed square, BI:Fo\_a = 1:1; open square, BI:Fo\_a = 4:3; closed circle, BI:Fo\_a = 2:1), (b) BI-Fo\_b (closed triangle, BI:Fo\_b = 1:2.3; open triangle, BI:Fo\_b = 1:2; closed square, BI:Fo\_b = 1:1.5; open square, BI:Fo\_b = 1:1; closed circle, BI:Fo\_b = 2:1), and (c) BI-Fo\_c (open triangle, BI:Fo\_c = 1:2; closed square, BI:Fo\_c = 1:1.5; open square, BI:Fo\_c = 1:1; closed circle, BI:Fo\_c = 2:1). Open circles in each panel indicate pure BI. Broken and dotted lines are the swelling limit and SmA-SmC phase transition temperature, respectively.

Figure 5 Layer thicknesses of the mixtures at various temperatures as a function of the volume fraction of the fluorinated oil  $\Phi_{Fo_a(b)}$ : (a) BI-Fo\_a, (b) BI-Fo\_b, and (c) BI-Fo\_c. Calculations were based on the method of [7]. The open symbols represent Iso-SmA macroscopic phase separation. (d) A schematic image of the swollen system composed of BI and straight-chain-like perfluorinated oils.

Figure 6 Conoscope images of SmA (80 °C) for (a) pure BI and (b) 33.3 wt% Fo\_b mixture.

Figure 7 Temperature dependence of (a) the optical birefringence  $\Delta n$  of pure BI and the 33.3 wt% Fo\_b mixture obtained from the conoscope figures and (b) the relative ratio of the  $\Delta n$  of the 33.3 wt% Fo\_b mixture to that of pure BI.

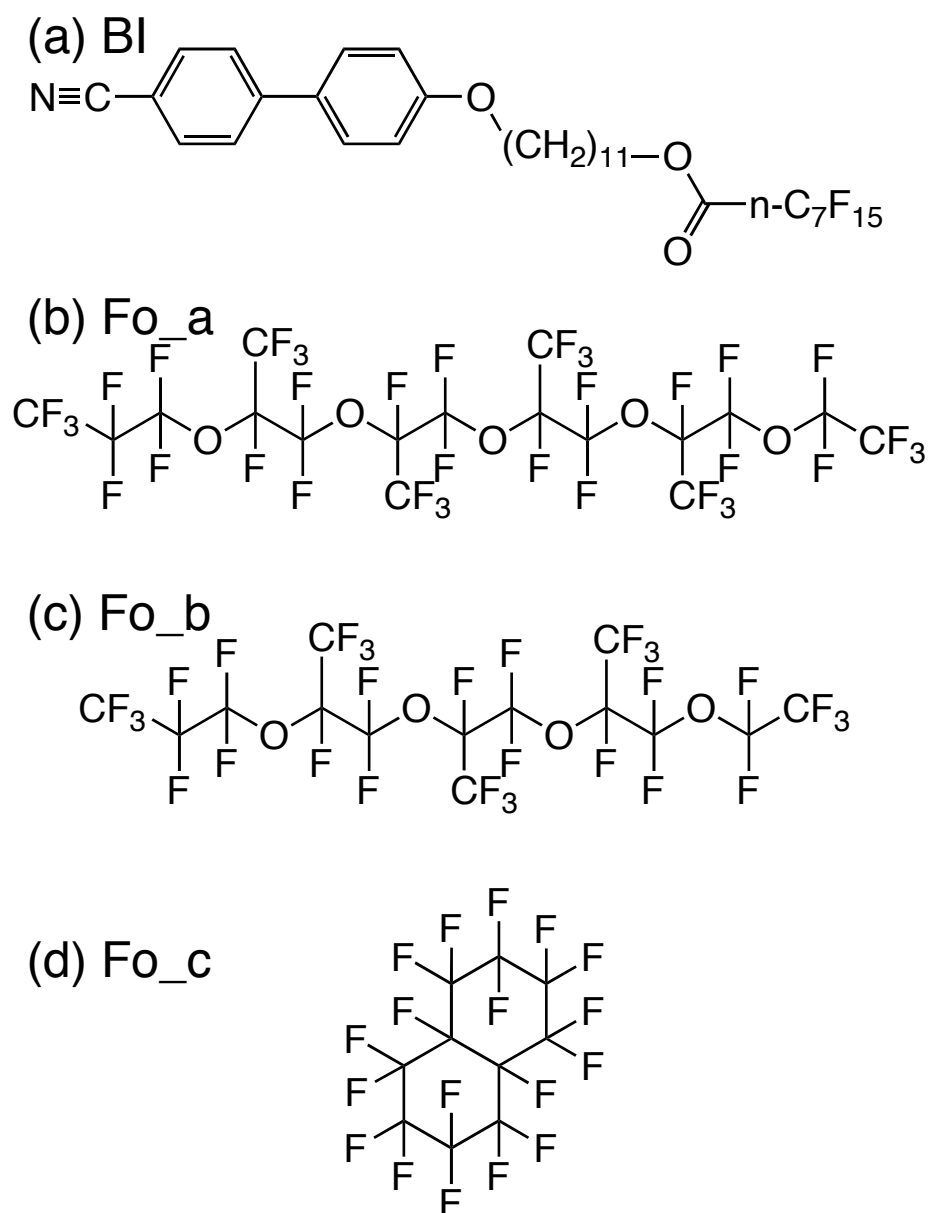


Fig.1 M. Murase et al.

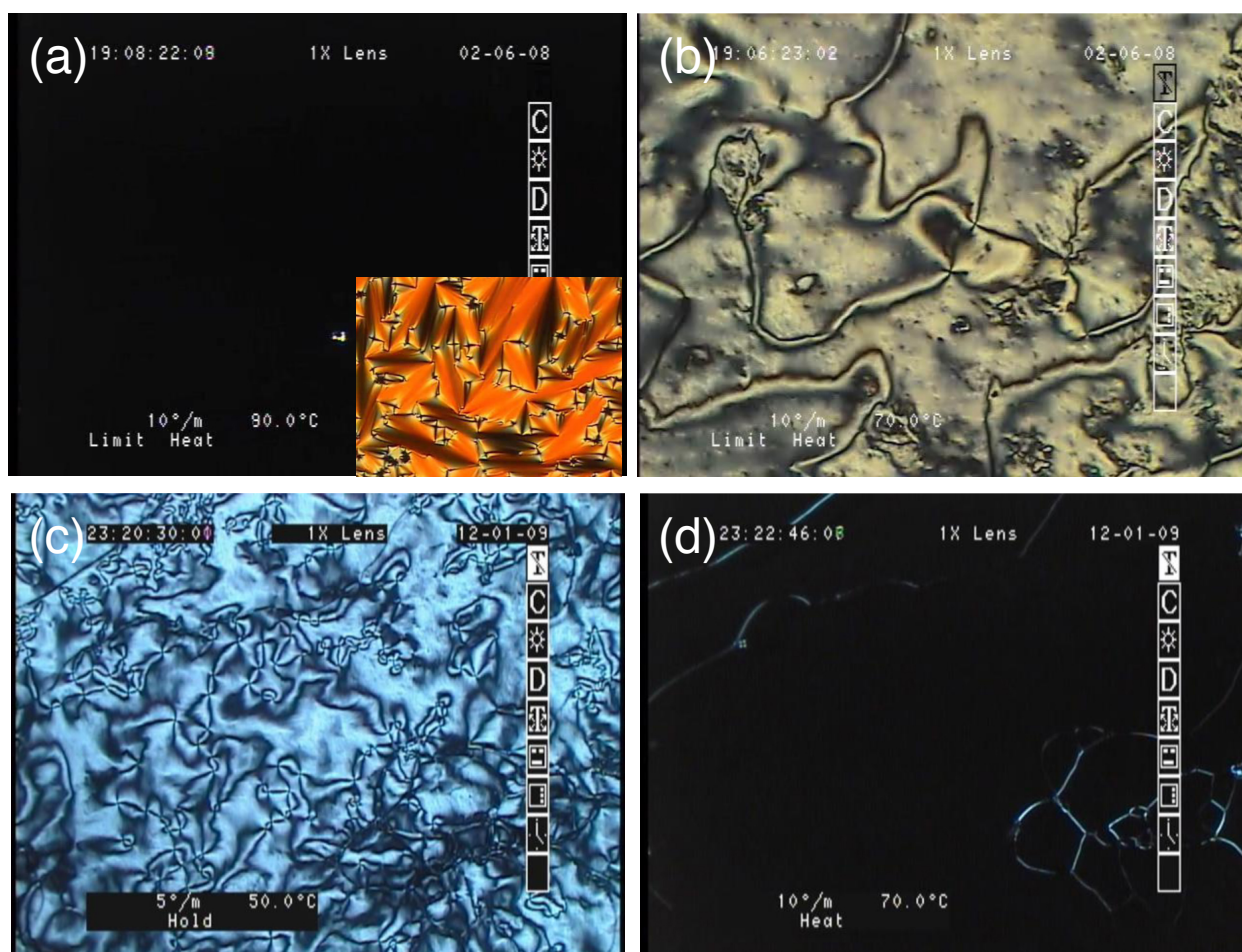


Fig.2 M. Murase et al.

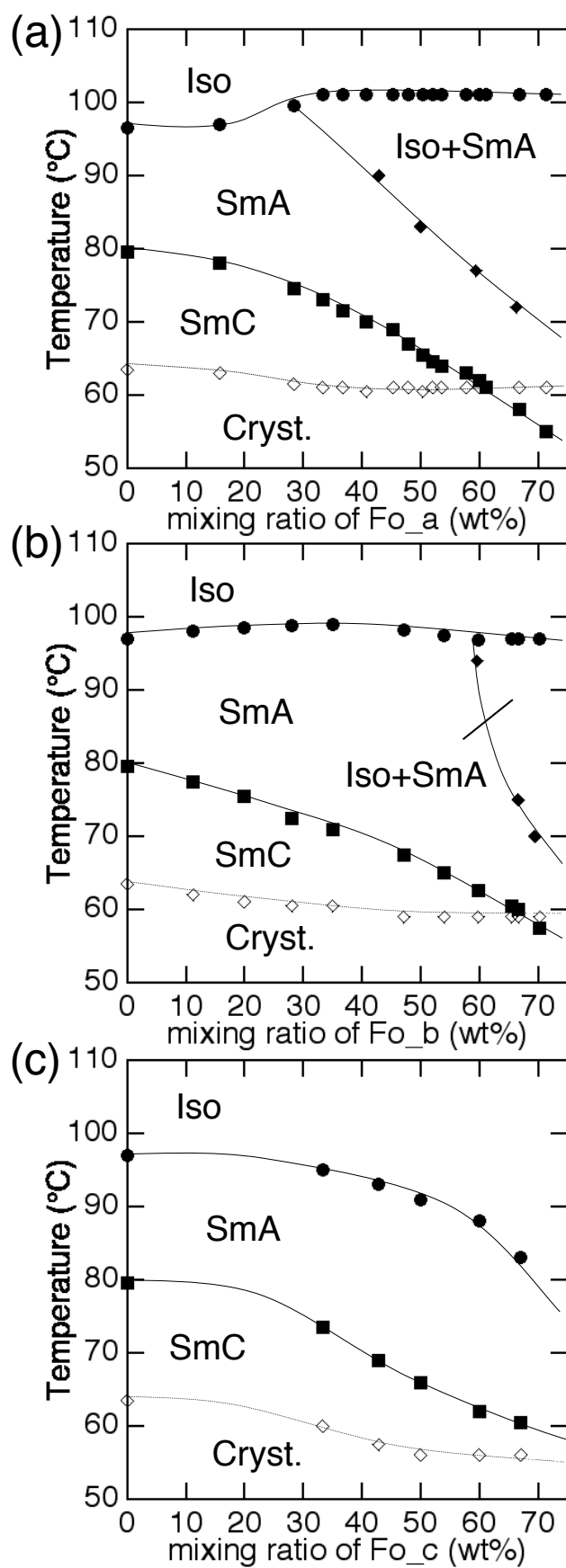


Fig.3 M. Murase et al.

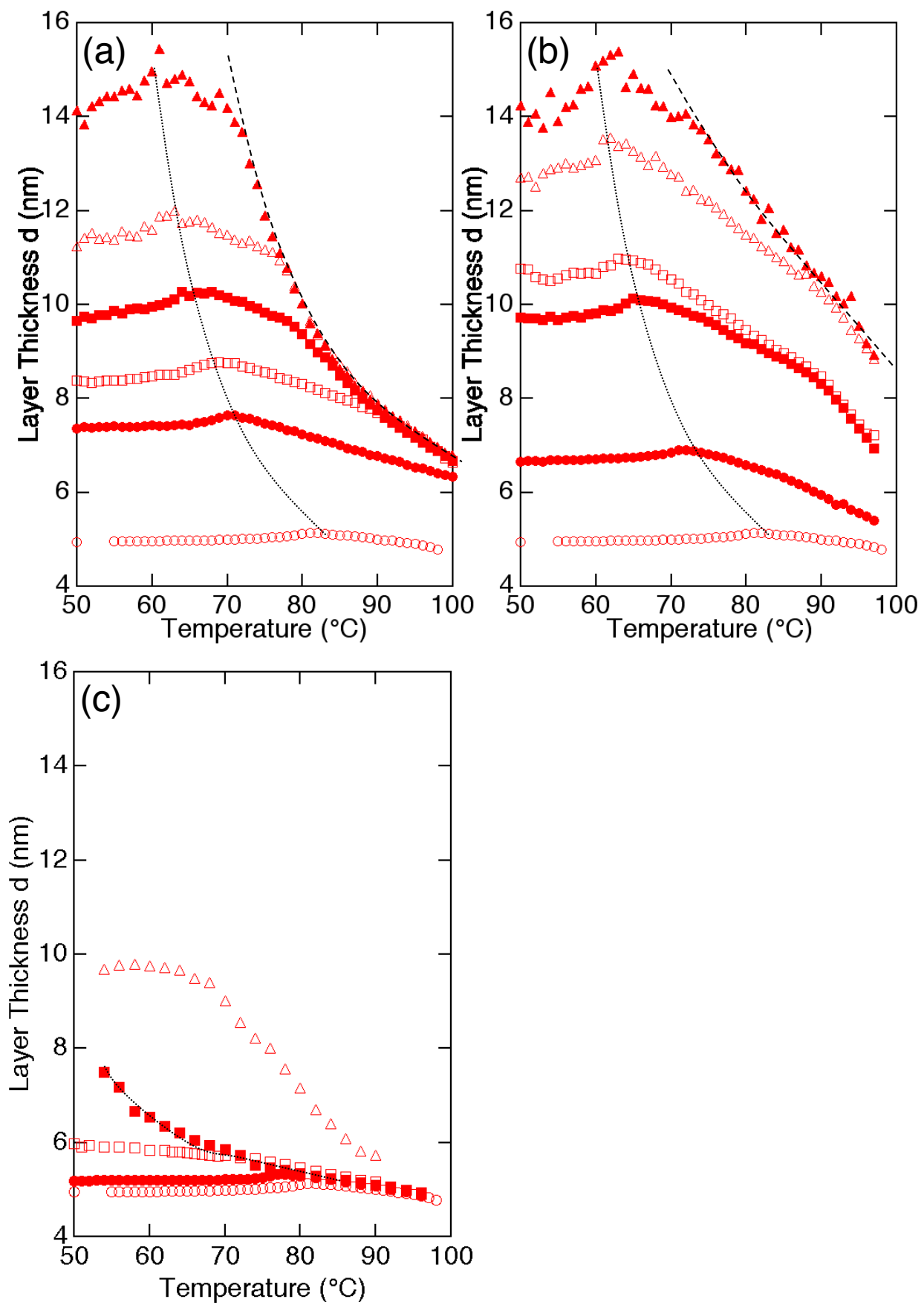


Fig.4 M. Murase et al.



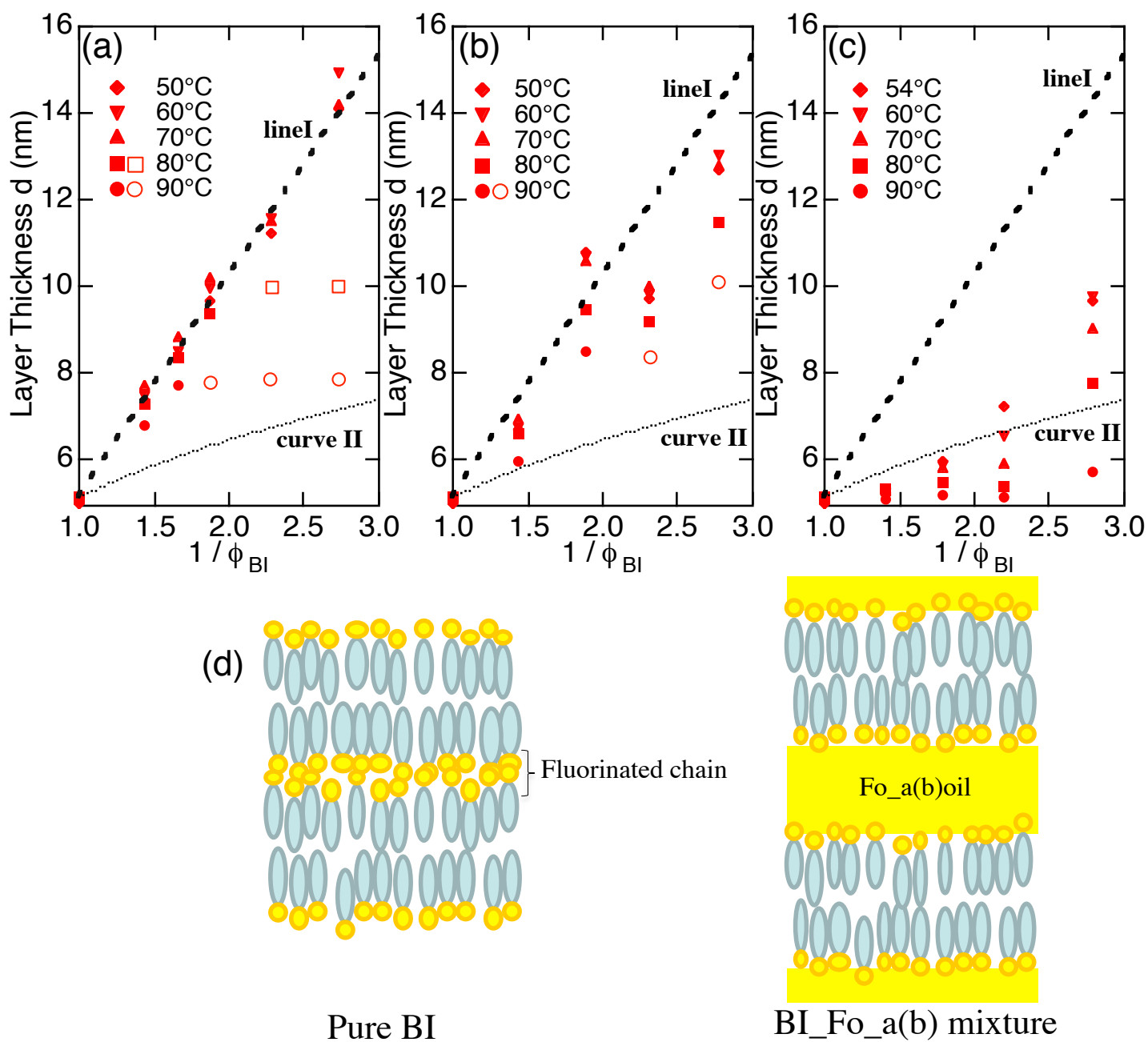


Fig.5 M. Murase et al.

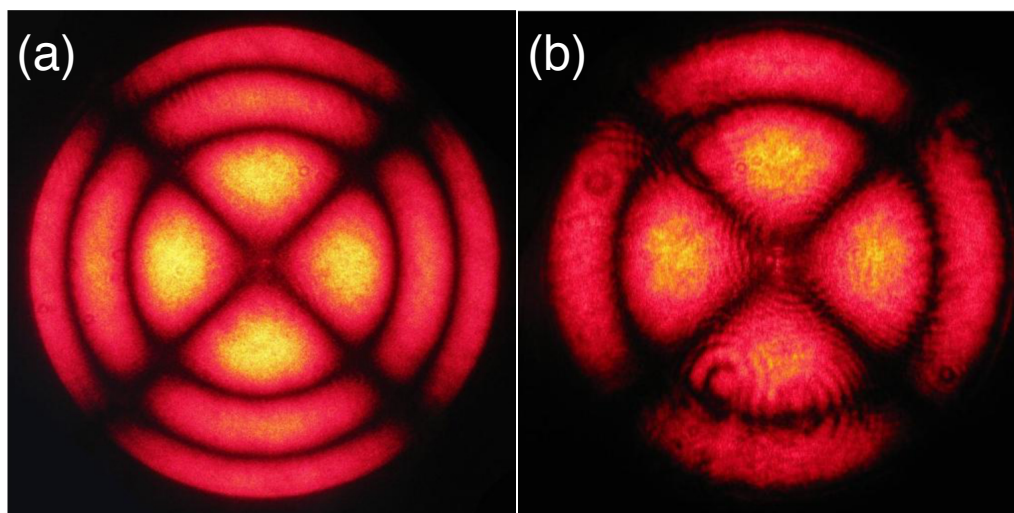


Fig.6 M. Murase et al.

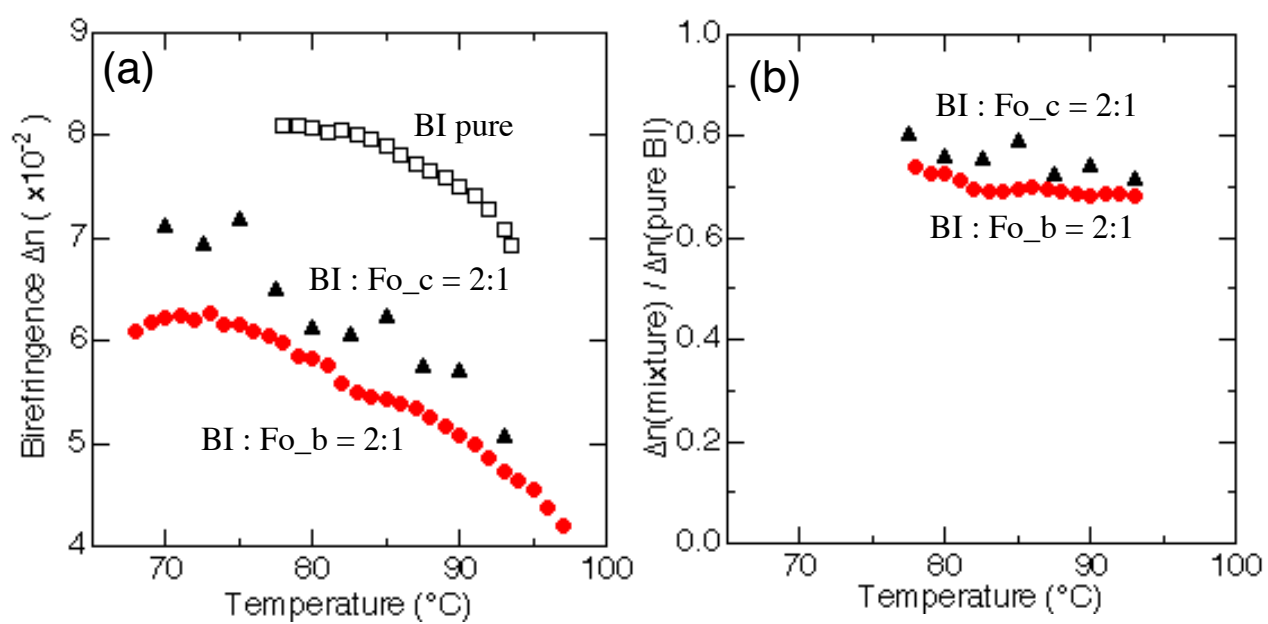


Fig.7 M. Murase et al.